Development ePress. Posted online 6 January 2015
 | Development (2015) 142, 1-11 doi:10.1242/dev.115931

RESEARCH ARTICLE

ERBB3-mediated regulation of Bergmann glia proliferation in cerebellar lamination

Anupama Sathyamurthy[1], Dong-Min Yin[1], Arnab Barik[1], Chengyong Shen[1,2], Jonathan C. Bean[1], Dwight Figueiredo[1,2], Jin-Xiong She[3], Wen-Cheng Xiong[1,2,4] and Lin Mei[1,2,4,*]

ABSTRACT

Cortical lamination is crucial for the assembly of cerebellar circuitry. In this process, granule neurons (GNs) migrate along Bergmann glia (BG), which are specialized astroglial cells, from the external granule layer to the internal granule layer. However, the molecular mechanisms underlying BG development are not well understood. Here, we show that *GFAP::Cre;Erbb3*$^{F/F}$ mice, which lack *Erbb3* in both radial glia and neurons, exhibit impairments in balance and motor coordination. Cerebellar lamination is aberrant, with misplaced Purkinje neurons and GN clusters. These phenotypes were not observed in *Math1::CreER*^{T2}*;Erbb3*$^{F/F}$ mice, where the *Erbb3* gene was deleted in GNs, suggesting involvement of non-neuronal *Erbb3* in cerebellar lamination. Mechanistic studies indicate that ERBB3 is crucial for the proliferation of BG, which are required for GN migration. These observations identify a crucial role for ERBB3 in cerebellar lamination and reveal a novel mechanism that regulates BG development.

KEY WORDS: Cerebellum, ERBB3, Bergmann glia, Mouse

INTRODUCTION

The cerebellum plays a key role in the neural control of motor movement. It has recently been implicated in higher order processes, including cognition (Buckner, 2013; Fatemi et al., 2012; Manni and Petrosini, 2004). Fundamental to cerebellar function is its unique laminar organization (Apps and Garwicz, 2005). The adult cerebellar cortex has three distinct layers: an outer molecular layer (ML), a middle Purkinje cell layer (PCL) and an internal granule layer (IGL) (Fig. 1A). Cell bodies of granule neurons (GNs) and Purkinje neurons (PNs) reside in the IGL and PCL, respectively, whereas axons of GNs synapse onto dendrites of PNs in the ML. The PCL also contains the soma of Bergmann glia (BG), which extend unipolar processes to contact the pial membrane and are important for cerebellar lamination (Rakic, 1971). During development, granule cell precursors (GCPs) proliferate in the external granule layer (EGL) beneath the glia limitans (formed by BG end feet) and migrate along the BG fibers into the IGL. Individuals with cerebellar cortical dysplasia exhibit GN heterotopia and loss of BG and clinical symptoms including ataxia, speech impairments and delays in motor and cognitive development (Laure-Kamionowska and Maslinska, 2007; Poretti et al., 2009; Rorke et al., 1968; Soto-Ares et al., 2000); however, underlying genetic mechanisms remain unclear. Although both GN and BG are crucial for lamination, in contrast to GN development, which has been studied extensively (Sotelo, 2004; Wang and Zoghbi, 2001), little is known about mechanisms that control BG development.

Neuregulins (NRG) comprise a large family of epidermal growth factor (EGF)-like proteins that are encoded by six different genes (Mei and Xiong, 2008; Mei and Nave, 2014). NRG1 has been implicated in neural development and brain activity homeostasis, although the function of other NRGs remains poorly understood. NRGs act by activating ERBB tyrosine kinases, including ERBB2, ERBB3 and ERBB4. ERBBs have been implicated in various aspects of neural development. *In vitro* analysis suggested that NRG1, via activating ERBB2 and ERBB4, induces glia differentiation that is necessary for radial migration of neurons in the cortex and cerebellum, respectively (Anton et al., 1997; Rio et al., 1997). However, ERBB2/ERBB4 double knockout has no effect on cortical and cerebellar lamination (Barros et al., 2009; Gajendran et al., 2009). On the other hand, ERBB4 is crucial for the assembly of GABAergic circuitry (Fazzari et al., 2010; Ting et al., 2011; Yang et al., 2013; Yin et al., 2013b; Bean et al., 2014), whereas ERBB3 is necessary for myelination in the CNS and PNS (Brinkmann et al., 2008; Lyons et al., 2005; Makinodan et al., 2012; Riethmacher et al., 1997). Although ERBB3 is expressed in the developing brain, its role in CNS development remains unknown due to embryonic lethality of null mutation (Erickson et al., 1997; Riethmacher et al., 1997).

In this study, we investigated the role of ERBB3 in cerebellar development by characterizing CNS-specific *Erbb3* mutant mice. *Erbb3* mutation in both BG and neurons led to GN dislocation. Mutant mice exhibited motor defects. These phenotypes were not observed in mice where the *Erbb3* gene was deleted in GNs, suggesting a necessary role for *Erbb3* in BG development. We investigated underlying mechanisms by characterizing mutant mice at different stages of cerebellar development. Results indicate that ERBB3 in BG plays a crucial role in cerebellar lamination.

RESULTS

Loss of ERBB3 in the brain causes motor impairments

To investigate whether ERBB3 plays a role in brain development, we characterized its expression by western blot analysis. As shown in Fig. 1B, ERBB3 was expressed in the brain as early as E16 and plateaued around P20. This temporal expression correlates with cerebellar lamination, which occurs from E15 to P21 (Goldowitz and Hamre, 1998). Embryonic lethality of *Erbb3*-null mice has precluded the study of the role of ERBB3 in cerebellar lamination (Erickson et al., 1997; Riethmacher et al., 1997). To circumvent this, we used Cre-Lox-based conditional knockout approach to knock out the *Erbb3* gene specifically in the CNS. Floxed *Erbb3*

[1]Department of Neuroscience and Regenerative Medicine, Medical College of Georgia, Georgia Regents University, Augusta, GA 30912, USA. [2]Charlie Norwood VA Medical Center, Augusta, GA 30904, USA. [3]Center for Biotechnology and Genomic Medicine, Medical College of Georgia, Georgia Regents University, Augusta, GA 30912, USA. [4]Department of Neurology, Medical College of Georgia, Georgia Regents University, Augusta, GA 30912, USA.

*Author for correspondence (lmei@gru.edu)

Received 29 July 2014; Accepted 27 November 2014

Development (2015) 142, 1-11 doi:10.1242/dev.115931

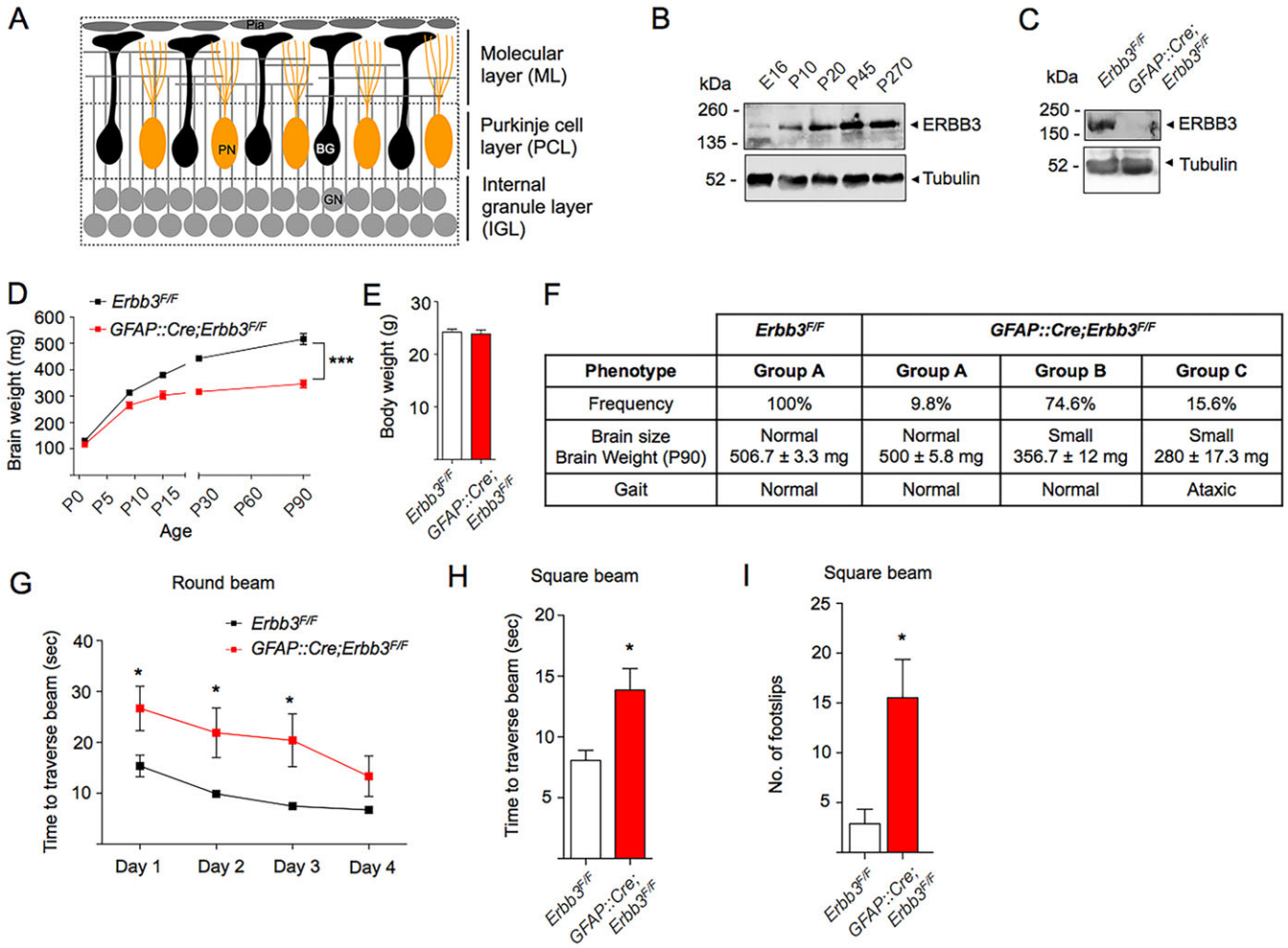

	Erbb3F/F	GFAP::Cre;Erbb3F/F		
Phenotype	**Group A**	**Group A**	**Group B**	**Group C**
Frequency	100%	9.8%	74.6%	15.6%
Brain size Brain Weight (P90)	Normal 506.7 ± 3.3 mg	Normal 500 ± 5.8 mg	Small 356.7 ± 12 mg	Small 280 ± 17.3 mg
Gait	Normal	Normal	Normal	Ataxic

Fig. 1. Motor deficits in *Erbb3* mutant mice. (A) Laminar structure of the cerebellar cortex. Major types of cells in different layers are: GNs in the IGL and PNs and BG in the PCL. The ML contains interneurons and synapses between GNs and PNs. BG extend unilateral processes, which contact meningeal cells in the pial surface. (B) Age-dependent increase in ERBB3 expression in the brain. Brain homogenates were blotted with indicated antibodies. (C) Reduced ERBB3 level in *GFAP::Cre;Erbb3*$^{F/F}$ (*Erbb3* mutant) mice. Brains homogenates from control (*Erbb3*$^{F/F}$) and mutant mice (3 months of age) were blotted as in B. Similar data were obtained from nine controls and nine mutants. (D) Reduced brain weight of *Erbb3* mutant mice. n=3 mice per genotype; genotype $F(1,21)=412.1$, ***$P<0.0001$; age $F(4,21)=594.8$, ***$P<0.0001$; genotype×age interaction $F(4,21)=41.7$, ***$P<0.0001$; two-way ANOVA followed by Bonferroni post-hoc test. (E) Similar body weight between control and *Erbb3* mutant mice. Data were collected at 3 months of age. n=7 and n=8 for control and mutant mice, respectively; $P=0.73$; t-test. (F) Classification of *Erbb3* mutant mice. Mice were grouped by brain size and gait (n=111 controls, 122 mutants). Data are presented as mean±s.e.m. (n=3 per group). (G) Increased round-beam crossing time in *Erbb3* mutant mice. Mice were allowed to cross a round beam (12 mm diameter, 1 m long) and latency was measured. n=9 and n=13 for control and mutant mice, respectively; genotype $F(1,20)=5.8$, *$P=0.03$; trial $F(3,60)=5.1$, **$P=0.003$; Genotype×trial interaction $F(3,60)=0.49$, $P=0.69$; two-way ANOVA (repeated measure) followed by Fisher's least significance difference test. (H) Increased square-beam crossing time in *Erbb3* mutant mice. Mice were allowed to cross a square beam (5 mm wide×80 cm long) and latency was measured. n=9 and n=10 for control and mutant mice, respectively; *$P=0.01$; t-test. (I) Mice were tested as in H and monitored for foot slips. More foot slips were recorded in *Erbb3* mutant mice. n=9 and n=10 for control and mutant mice, respectively; *$P=0.01$; t-test. In D-I, data are mean±s.e.m.

mice (Qu et al., 2006) were crossed with *GFAP::Cre* mice (Zhuo et al., 2001). Cre expression in *GFAP::Cre* mice occurs as early as E13.5 in precursor cells in the cerebellum that give rise to both GNs and glia. Resulting *GFAP::Cre;Erbb3*$^{F/F}$ mice (hereafter referred to as *Erbb3* mutants) were vital at birth and showed reduced expression of ERBB3 in the brain (Fig. 1C; supplementary material Fig. S1A).

At birth, *Erbb3* mutant mice appeared normal, had normal brain mass and were indistinguishable from control mice. However, as they aged, mutants showed a smaller increase in brain weight than controls (Fig. 1D). Approximately 90% of mutant mice had significantly smaller brains than controls. There was no difference in body weight between control and mutant mice as late as P90 (Fig. 1E), suggesting that reduction in brain weight was not secondary to body weight reduction. Intriguingly, ataxic gait was observed in 15.6% of the *Erbb3* mutants, but not in any of the control mice (supplementary material Movie 1). Based on brain size and gait, mutants could be classified into three groups: group A with normal brain size and gait; group B with smaller brain and normal gait; and group C with smaller brain and ataxic gait (Fig. 1F; supplementary material Fig. S1B).

Next, we determined whether the mutants without obvious gait abnormality were impaired in motor skills. Mice were subjected to elevated beam-walk assays on round or square beams. The amount of time taken to cross the beam and the number of foot slips were quantified. On the first day of trial, control mice crossed the round beam in 15.4±2.1 s (n=9), whereas mutants took significantly longer to cross the beam (Fig. 1G). Both controls and mutants

Development (2015) 142, 1-11 doi:10.1242/dev.115931

improved over time, and on day 4, the difference in latency was insignificant. On day 5, when mice were challenged on a narrower, square beam, mutants performed worse than controls (Fig. 1H). The mutants also displayed more foot slips of the hind paw (Fig. 1I; supplementary material Fig. S1C). These results indicate that *Erbb3* mutant mice have impaired motor skills, suggesting that brain regions involved in motor control and coordination might be altered by *Erbb3* mutation.

The cerebellum fails to laminate normally in the absence of ERBB3

Motor impairments are often caused by disorders of the cerebellum (Manni and Petrosini, 2004). The findings that *GFAP::Cre*;*Erbb3*$^{F/F}$ mutants displayed ataxia and motor defects suggested that the structure and/or function of cerebella were altered. To test this hypothesis, we carried out morphological examination of Nissl-stained cerebellum. At P3, gross anatomy and volume of cerebellum were similar between control and *Erbb3* mutant mice (Fig. 2A,B). Although the thickness of the EGL was similar, the fissures that extend between adjacent folia were shorter in mutants (Fig. 2C,D). The EGL and IGL were readily visible at P9 in control and *Erbb3* mutant cerebella. However, the EGL and IGL were poorly defined and not easily distinguishable in mutant mice (Fig. 2A). At P30 and P90, most GCPs in the EGL had migrated into the IGL in control mice and thus replaced by the ML. The cerebellum had fully developed folia, and the boundary between the ML and IGL was well defined. In *Erbb3* mutants, however, adjacent cerebellar folia appeared to be fused and the boundary between the ML and IGL was ill defined. Ectopic clusters of cells were visible in the ML layer, most likely GNs that had failed to migrate into the IGL (Fig. 2A,G, arrow; supplementary material Fig. S2A,E). At P30 and P90, ectopic clusters occupied ∼3-4% of the molecular layer in mutants (<0.004% in controls). The cerebella of *Erbb3* mutants were smaller at P9, P30 and P90, but not at P3 when the cerebellar cortex starts to develop (Fig. 2A,B,E; supplementary material Fig. S2A-C). In group C *Erbb3* mutant mice, which exhibited ataxia (Fig. 1F), cerebellar lamination deficits appeared to be more severe: adjacent folia were not well demarcated. The area occupied by ectopic clusters was greater in group C *Erbb3* mutants compared with group B mutants (supplementary material Fig. S2A,B,E).

During cerebellar lamination, GCPs proliferate in the outer region of the EGL and thus are positive for Ki67, a proliferation marker (Li et al., 2013). After mitotic division, GCPs differentiate into immature GNs, which accumulate in the inner EGL and are Tuj1+ (Qu and Smith, 2005). Subsequently, immature GNs migrate to the IGL, where they become mature GNs and express

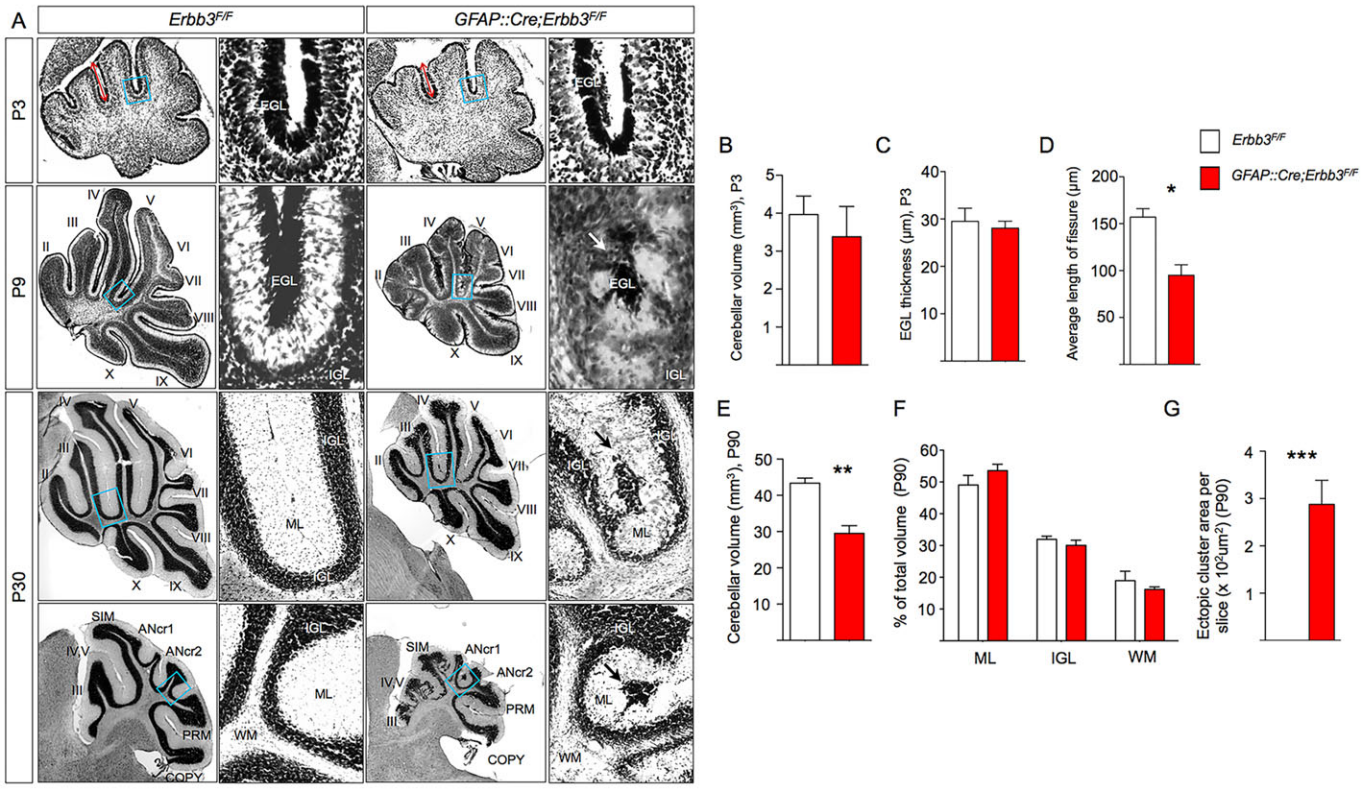

Fig. 2. Abnormal cerebellar lamination in *Erbb3* mutant mice. (A) Brains were isolated from mice after transcardial perfusion with 4% PFA. Sagittal sections of the cerebellum were subjected to Cresyl Violet staining. Columns 2 and 4 are higher magnification views of areas framed in respective low-magnification images in columns 1 and 3. Ectopic clusters of GNs (arrows) were observed along the fusion lines of adjacent folia. Ectopic clusters were observed in all group B mutants (n=30 controls and 28 mutants, ages P7 to P100). (B,C) Similar cerebellar volume and EGL thickness at P3 in control and mutant. Every sixth coronal section of the cerebellum (35 µm) was subjected to Cresyl Violet staining; area, thickness and spacing of slices were used to estimate volume of the cerebellum. n=3 cerebella per group; P=0.57 (B) and P=0.68 (C), respectively; t-test. (D) Reduced fissure length at P3 in *Erbb3* mutants. Cerebellar sections were stained as in B. Every sixth coronal section was used to measure the average fissure length per cerebella. n=3 cerebella per group; *P=0.01; t-test. (E) Reduced cerebellar volume at P90 in *Erbb3* mutants. Cerebellar volume was determined as in B. n=3 cerebella per group; **P=0.006; t-test. (F) Relative volume of ML, IGL and WM. n=3 cerebellar per group; P>0.05; t-test. (G) Quantification of area occupied by ectopic clusters. Cerebellar sections were stained as in E. Every sixth cerebellar section was analyzed to determine the area occupied by ectopic clusters. n=31 and n=29 slices from three controls and three mutants, respectively; ***P<0.0001; t-test.

Development (2015) 142, 1-11 doi:10.1242/dev.115931

NeuN (Weyer and Schilling, 2003). To investigate cellular mechanisms underlying aberrant cerebellar lamination in *Erbb3* mutants, P9 cerebella were stained for Ki67, Tuj1 and NeuN. In control mice, Ki67+ GCPs of the outer EGL were in close apposition to the pial membrane that extended into the fissures between adjacent folia (Fig. 3A). Beneath the outer EGL were post-mitotic, Tuj1+ immature GNs (Fig. 3A). By contrast, in *Erbb3* mutants, the boundary between the outer and inner EGL was ill defined and Ki67+ GCPs were interspersed among immature GNs in both inner and outer EGL (Fig. 3A). In control mice, mature NeuN+ GNs were confined to the IGL (Fig. 3B). However, in *Erbb3* mutants, mature NeuN+ GNs failed to reach the IGL, but instead clustered in the EGL and in areas between the EGL and IGL. These results suggest that ERBB3 plays a role in GN migration. Besides GNs, we examined PNs, another major type of neuron in the cerebellum, which could be labeled by calbindin (Celio, 1990). In control mice, the soma of calbindin+ cells were restricted to the PCL of the cerebellar cortex (Fig. 3C), whereas in mutants, they were not confined to the PCL. Because the Cre in *GFAP::Cre* mice was expressed in precursor cells that give rise to GNs and glia, but not PNs in the cerebellum (Spassky et al., 2008; Zhuo et al., 2001), PN mislocation may be secondary to cerebellar lamination abnormality stemming from ERBB3 deficiency in other cells.

Neuronal *Erbb3* is dispensable for cerebellar lamination

Proliferation and migration of GCPs depend on two cell intrinsic factors: (1) the ability of GCPs to adhere extracellular matrix (ECM) proteins in the basement membrane; and (2) the ability of GNs to extend neurites (Komuro and Yacubova, 2003; Sotelo, 2004). Mutation of genes that regulate GCP adhesion or GN neurite outgrowth result in mislocation of GNs and laminar defects of the cerebellum (Engelkamp et al., 1999; Koirala et al., 2009; Peng et al., 2010). The attachment of *GFAP::Cre;Erbb3*$^{F/F}$ GCPs to laminin-coated coverslips was similar to that of control GCPs (Fig. 4A,B), suggesting normal adhesion of mutant GCPs to the ECM. Neurite extension was apparently normal in GNs from *GFAP::Cre;Erbb3*$^{F/F}$ mice, compared with those from controls (Fig. 4C,D). These results suggest that GN misplacement in *GFAP::Cre;Erbb3*$^{F/F}$ mice may not be due to GCP adhesion or to GN neurite outgrowth. To further test this hypothesis, we selectively ablated *Erbb3* in GCPs that give rise to GNs. Math1 (Atoh1 – Mouse Genome Informatics) is a transcription factor that is expressed in GCPs in the rhombic lip and EGL, as well as neurons in nuclei of the hindbrain and midbrain (Ben-Arie et al., 1997). *Erbb3*$^{F/F}$ mice were crossed with *Math1::CreER*^{T2} mice; pregnant dams were injected with tamoxifen at E15, a time when the Cre is induced only in GCPs (Machold and Fishell, 2005). However, *Erbb3* deletion (supplementary material Fig. S3A,B) by *Math1::CreER*^{T2} did not appear to alter ERBB3 levels

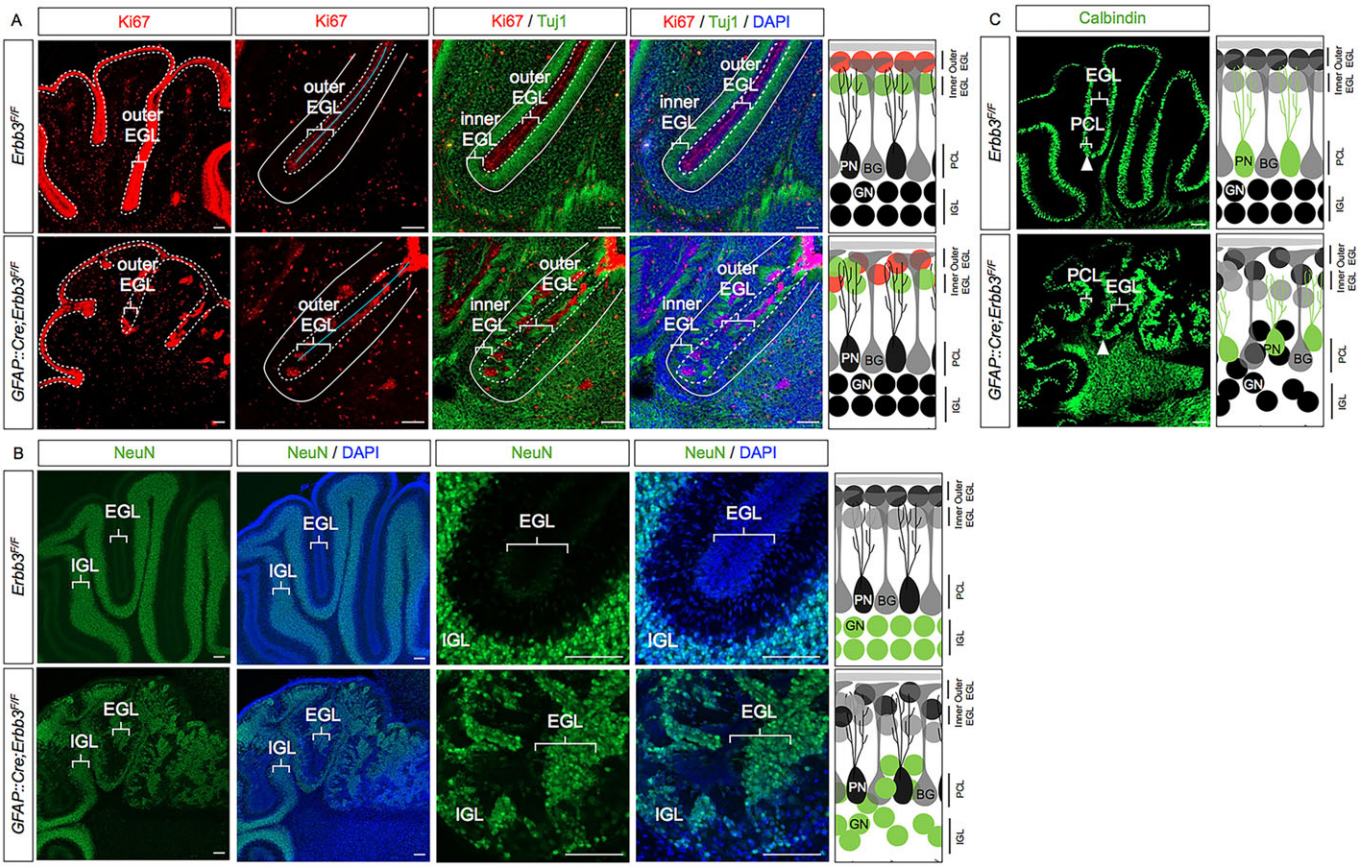

Fig. 3. Mislocation of granule neurons and Purkinje neurons in the cerebella of *Erbb3* mutant mice. Immunostaining of P9 coronal sections from control and mutant mice with indicated antibodies. (A) Ill-defined boundary between outer and inner EGLs. Sections were stained with antibodies against Ki67 (to label GCPs) and Tuj1 (for migrating GNs). Outer EGL is between dashed lines, whereas inner EGL is area between solid and dashed white lines. Solid blue line indicates the pial surface. (B) Presence of mature GNs in the EGL and in areas between the EGL and IGL. Sections were stained with anti-NeuN antibody to label mature GNs. (C) Misalignment of PN soma in mutant cerebellum. Sections were stained with anti-calbindin antibody (to label PNs). Solid white arrowheads indicate the soma of PNs. Pictographs on the right illustrate immunostained cells and cerebellar morphology. Data are representative of results obtained from five mice per group. Scale bars: 100 µm.

Development (2015) 142, 1-11 doi:10.1242/dev.115931

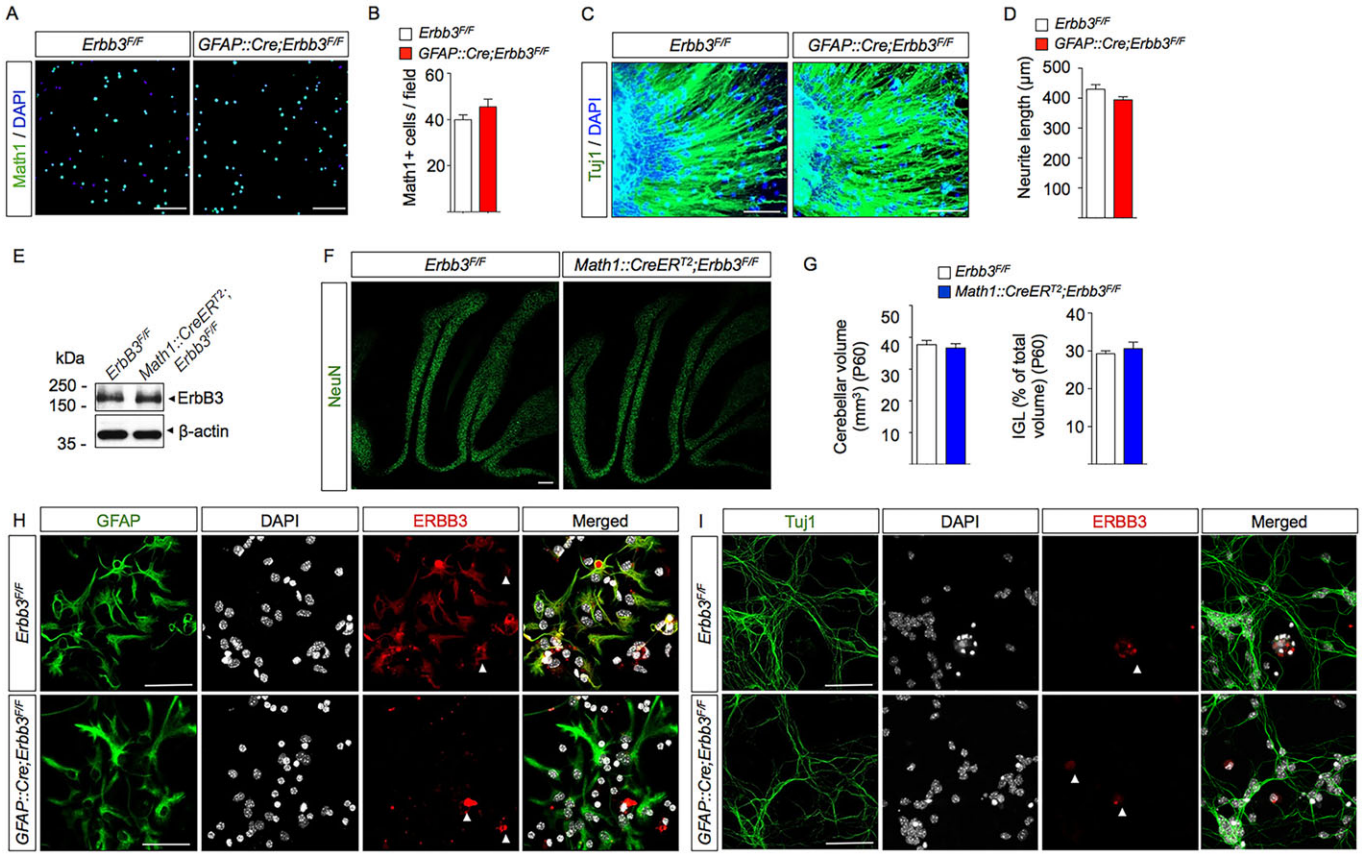

Fig. 4. Normal cerebellar lamination in granule neuron-specific *Erbb3* mutant mice. (A) Similar number of control and *Erbb3* mutant Math1+ cells adhered to laminin. Granule cells from P0 pups (four pups per group) were plated in dishes coated with laminin for 2 h. Shown are images of Math1-staining. Scale bars: 100 µm. (B) Quantification of Math1+ cells in A. n=15 fields for controls and mutants; P=0.17; t-test. (C) Similar neurite outgrowth in cerebellar explants in control and *GFAP::Cre;Erbb3*$^{F/F}$ mice. Cerebellar explants from P0 mice (four pups per group) were cultured *in vitro* for 2 days. Shown are images of Tuj1 staining. Scale bars: 100 µm. (D) Quantification of neurite length in A. n=26 and n=25 explants for controls and mutants, respectively; P=0.07; t-test. (E) Similar ERBB3 levels in cerebellar lysates of control and *Math1::CreER*^{T2}*;Erbb3*$^{F/F}$ mice. Pregnant dams (at E15) carrying control and *Math1::CreER*^{T2}*;Erbb3*$^{F/F}$ embryos were injected with tamoxifen (i.p.). P30 mice were sacrificed and cerebella were isolated for western blot. Similar data were obtained from four controls and four mutants. (F) Normal cerebellar lamination in *Math1::CreER*^{T2}*;Erbb3*$^{F/F}$ mice. Expression of Cre was induced as in E. Sections were stained with anti-NeuN antibody. Data are representative of results obtained from eight mice per group. Scale bar: 200 µm. (G) Quantification of cerebellar volume and relative volume occupied by IGL at P60. Every fifth cerebellar section was analyzed to determine the area occupied by the IGL. Area, thickness and spacing of slices were used to estimate volume. n=3 cerebella per group; P>0.05; t-test. (H,I) ERBB3 expression in GFAP+ cerebellar astroglial cells. Cerebellar astrocytes (H) and neurons (I) were cultured from control and *GFAP::Cre;Erbb3*$^{F/F}$ mice, and at DIV4 (astrocytes) or DIV7 (granule neurons) they were subjected to immunostaining with anti-ERBB3 and anti-GFAP or anti-Tuj1 antibodies. ERBB3 was detected in control GFAP+ glial cells, but not mutant GFAP+ glial cells, control Tuj1+ cells or mutant Tuj1+ cells. White arrowheads indicate cells that express ERBB3 but not GFAP (H) or Tuj1 (I). Scale bars: 50 µm. In B,D,G, data are mean±s.e.m.

in the cerebellum (Fig. 4E), indicating that ERBB3 was not expressed in GCPs or in GNs. In agreement, cerebellar size or morphology in *Math1::CreER*^{T2}*;Erbb3*$^{F/F}$ mutants showed no difference from that of control mice after tamoxifen injection (Fig. 4F,G). Unlike *GFAP::Cre;Erbb3*$^{F/F}$ mutants, ectopic clusters of NeuN+ GNs were not observed in the ML of *Math1::CreER*^{T2}*;Erbb3*$^{F/F}$ mice. Instead, NeuN+ GNs were localized in the IGL, as observed in control mice. In addition, staining with GFAP, an intermediate filament protein, showed no difference between tamoxifen-injected control and *Math1::CreER*^{T2}*;Erbb3*$^{F/F}$ mutants (supplementary material Fig. S3C), suggesting that the *Erbb3* gene in GCPs or GNs was not required for BG development or maintenance. Together, these observations indicate that lack of the *Erbb3* gene in GCPs or GNs has no effect on cerebellar cortical lamination.

Glial scaffolding abnormalities in *Erbb3* mutant mice

The above results suggest that the phenotypes in *Erbb3* mutants may be due to lack of *Erbb3* in glial cells in the cerebellum. Cerebellar glial cells, including BG, are derived from glial precursors in the ventricular zone of the fourth ventricle and express GFAP (Bignami and Dahl, 1973; Yamada and Watanabe, 2002). We determined whether ERBB3 was expressed in astroglial cells of the cerebellum. Astroglial cells were cultured and subjected to immunostaining with anti-ERBB3 and -GFAP antibodies. As shown in Fig. 4H, the purified cells were positive for GFAP, an astroglial marker, and thus were astroglial cells. ERBB3 was detected in all GFAP+ astroglial cells (Fig. 4H). Remarkably, ERBB3 immunostaining was absent in astrocytes purified from the cerebella of *GFAP::Cre;Erbb3*$^{F/F}$ mice. Moreover, ERBB3 was undetectable in Tuj1+ GNs in control or *GFAP::Cre;Erbb3*$^{F/F}$, consistent with our observation that loss of *Erbb3* in granule neurons did not affect cerebellar lamination (Fig. 4I). These results indicate that ERBB3 is expressed in cerebellar astrocytes, but not GNs (Fig. 4H,I). Occasionally, a small number of cells were found to express ERBB3, but not GFAP or Tuj1 (Fig. 4H,I, arrowhead). Most likely they were fibroblasts because their expression of ERBB3 was not altered by *Erbb3* mutation.

Development (2015) 142, 1-11 doi:10.1242/dev.115931

During development, unipolar BG extend processes to the pial surface; immature GNs migrate on these processes from the EGL to the IGL (Rakic, 1971). Genetic ablation of cerebellar astrocytes, including BG, at P1 leads to smaller cerebellum, GN and PN mis-positioning and severe ataxia (Cui et al., 2001; Delaney et al., 1996). Because *Erbb3* mutants exhibited similar phenotypes and because ERBB3 is expressed in cerebellar astroglial cells, we characterized BG morphology in *Erbb3* mutants. Cerebellar coronal sections were stained with anti-GFAP antibody to visualize BG cytoskeleton. In cerebella of P9 control mice, GFAP+ astrocytes were present in the white matter (Fig. 5). BG, which are located in the PCL, extended parallel processes to the pial surface, forming glial scaffolds. Their endfeet were in close apposition to the pial surface, forming glia limitans (Fig. 5, arrowhead). However, in *Erbb3* mutants, there was a significant reduction in GFAP staining in the white matter. Remarkably, the glial scaffolds were severely disorganized and failed to form glia limitans at P9. Similar deficits were observed in P90 mutant mice (supplementary material Fig. S4).

The disorganized glial scaffolds may be caused by the inability of *Erbb3* mutant BG to form a scaffold. Alternatively, it could be due to reduced numbers of BG. To determine whether *Erbb3* mutant cerebellar astroglial cells were able to form radial glial scaffold, we analyzed their morphology in culture by performing BLBP immunostaining. BLBP is expressed in most cerebellar astrocytes, including Bergmann glia (Feng et al., 1994). Under normal conditions, the percentage of control and mutant cells that displayed radial glial morphology (supplementary material Fig. S5A, yellow arrowhead) was similar. A previous study has shown that NRG1 can induce radial glial morphology in cultured cerebellar astrocytes (Rio et al., 1997). In control cells, NRG1 treatment induced radial glial morphology in a dose-dependent manner. This effect of NRG1 was not abolished in *Erbb3* mutant cerebellar astroglial cells (supplementary material Fig. S5A). Together, these results suggest that ERBB3 is dispensable for scaffold formation by cerebellar astroglial cells.

BG reduction in *Erbb3* mutant cerebellum

To determine whether inadequate scaffolding was due to reduced number of BG, we performed BLBP immunostaining to visualize BG at different stages of BG development. Around E15, there is an acceleration in BG migration from the ventricular zone of the fourth ventricle, where they are generated, to final destination in the PCL (Yamada and Watanabe, 2002). Once BG reach the PCL, they proliferate in the growing PCL. This proliferative activity of BG during the perinatal period is important for cerebellar development (Delaney et al., 1996). In order to determine whether embryonic generation and migration of BG was normal in mutants, we performed BLBP immunostaining at E18.5. As shown in Fig. 6A, the number of BLBP+ cells in the PCL was similar between controls and mutants at E18.5, suggesting that generation and migration of BG was not altered in mutants. In P9 cerebellar slices of control mice, the soma of BG were present in the PCL layer. They appeared to extend processes towards the pial membrane (Fig. 6B). However in P9 *Erbb3* mutants, BG soma were conspicuously absent in the PCL, and there were no well-defined glial scaffolds. Similar results were obtained by immunostaining for S100β, a cytoplasmic protein that is expressed in cerebellar glial cells, including cerebellar astrocytes and BG (Fig. 6C). These results indicate that the number of BG cells was reduced in *Erbb3* mutant cerebellum. Next, we isolated cerebellar astroglial cells from control and mutant cerebella, and analyzed their ability to expand in culture (Fig. 6D,E). The number of mutant cerebellar astroglial cells was only 50% of control at DIV12. Together, these data suggest that *Erbb3* ablation impairs the expansion of cerebellar glial cells.

Reduction in astroglial number could either be due to increased apoptosis or to reduced proliferation of astroglial cells. To determine whether *Erbb3* ablation alters the apoptosis of cerebellar astroglial cells, we performed TUNEL and GFAP staining to visualize apoptotic astroglial cells. As shown in supplementary material Fig. S5B, TUNEL-labeled GFAP+ cells were similar between control and mutant mice, suggesting little effect of *Erbb3* ablation on apoptosis of cerebellar astroglial cells. We next determined whether ERBB3 is

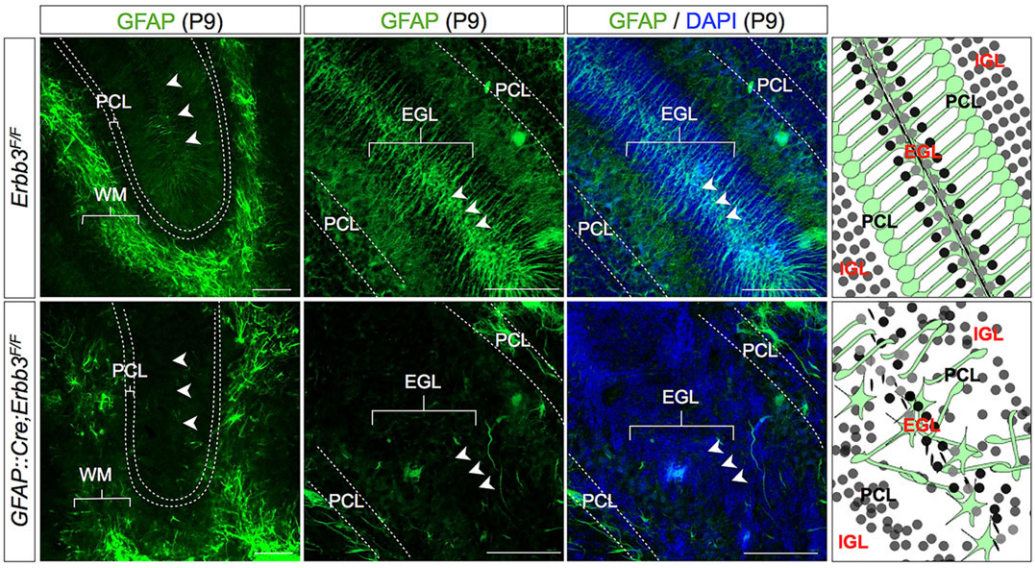

Fig. 5. Bergman glial scaffolds were disrupted in *Erbb3* mutant cerebellum. P9 coronal sections were stained with anti-GFAP antibody to label cerebellar astrocytes, including BG. In controls, end feet of BG were in close apposition to meningeal cell membrane and formed a continuous glia limitans (arrowheads). In mutants, the well-defined BG scaffold was absent and the glia limitans was discontinuous. Data are representative of results obtained from five mice per group. Scale bars: 100 µm. Pictographs on the right illustrate BG and cerebellar morphology.

Development (2015) 142, 1-11 doi:10.1242/dev.115931

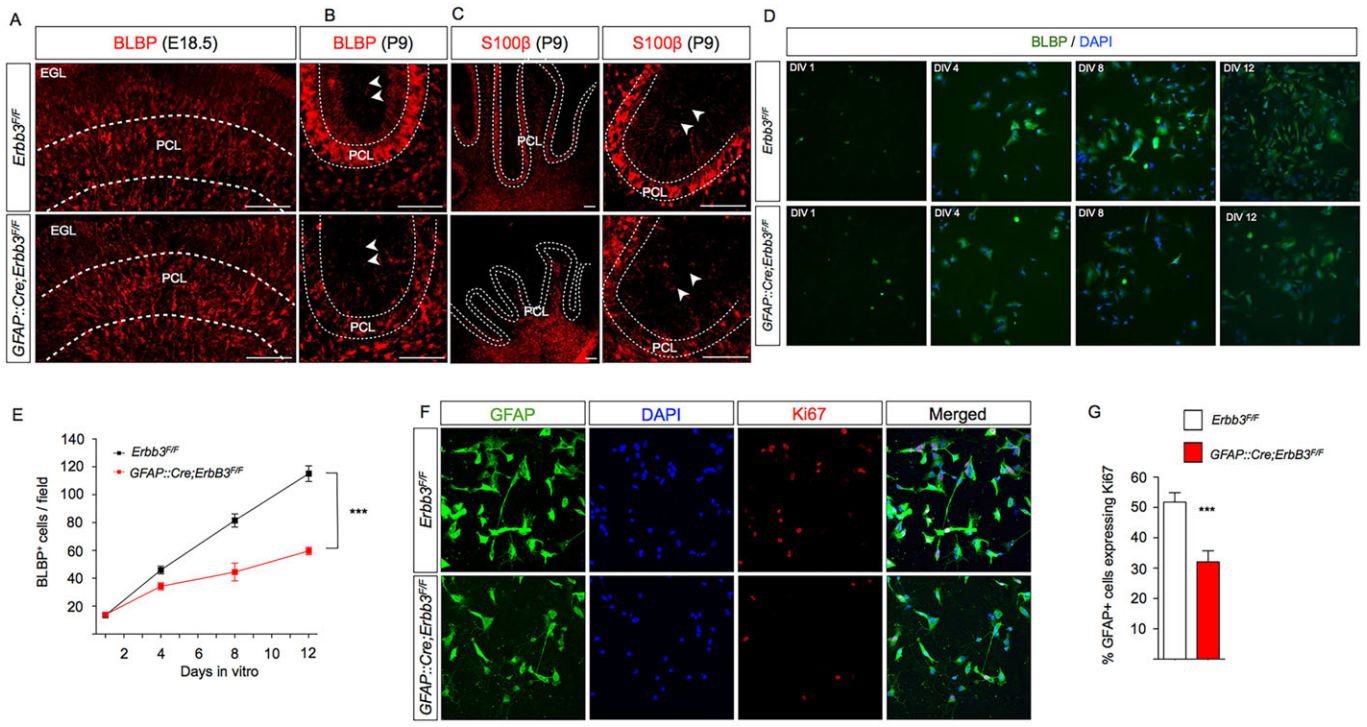

Fig. 6. Bergman glial cell number reduction in *Erbb3* mutant cerebellum. (A) Normal BLBP staining in PCL at E18.5. Coronal cerebellar sections of control and mutant embryos were immunostained with anti-BLBP antibody to visualize BG. Data are representative of results obtained from three embryos per group. Scale bars: 100 µm. (B,C) Reduction in BLBP+ cell number and S100β+ in PCL of *Erbb3* mutant mice. Coronal cerebellar sections from control and mutant mice (P9) were immunostained with indicated antibodies. PCL is outlined by dashed white lines. White arrowhead indicates glia limitans. The right column shows images at high magnification (C). Data are representative of results obtained from four mice per group. Scale bar: 100 µm. (D,E) Reduction in astroglial cell number *in vitro*. Cerebellar astroglial cells were cultured from control and mutant mice (5-6 pups per group) and subjected to BLBP immunostaining at indicated times. BLBP+ cells were quantified. n=15 images per time point; genotype $F(1,112)=90.9$, ***$P<0.0001$; time $F(3,112)=134.5$, ***$P<0.0001$; genotype×time interaction $F(3,112)=21.3$; ***$P<0.0001$; two-way ANOVA. (F,G) Reduced proliferation of *Erbb3* mutant astroglial cells. Cerebellar astroglial cells were cultured from control and mutant mice (four to six pups per group) and subjected to GFAP and Ki67 immunostaining at DIV5. The percentage of GFAP+ cells that expressed Ki67 was quantified (n=13 images for controls, 15 images for mutants; ***$P<0.001$; t-test). In E,G, data are mean±s.e.m.

necessary for astroglial proliferation. Cerebellar astroglial cells were subjected to staining with antibodies against GFAP and Ki67, a proliferation marker. Compared with control, fewer GFAP+ mutant astroglial cells expressed Ki67 (Fig. 6F,G), indicating that the proliferation of cerebellar astroglial cells requires ERBB3. Together, these data suggest that reduced number of mutant *Erbb3* cerebellar astroglial cells results from impaired proliferation, but not from increased cell death.

The number of TUNEL-labeled cells in the PCL was similar between control and *Erbb3* mutant mice (Fig. 7A), in agreement with the notion that the reduction in the number of BG in mutants was not due to compromised BG survival. To determine whether BG proliferation was reduced *in vivo* in *Erbb3* mutant mice, we determined the number of proliferating, Ki67+ glial cells in the PCL at different ages. In the PCL, BG are mitotic and thus Ki67+, whereas PNs are post-mitotic and should not be labeled by Ki67. As shown in Fig. 7B,C, the number of Ki67+ BG in the PCL was significantly reduced in the mutants as early as E18.5 (27.7±4.6% of controls). These Ki67+ cells in the PCL also expressed nestin, an intermediate filament protein expressed in cerebellar astroglial cells, including BG (supplementary material Fig. S5C). At P0.5, proliferating BG were further reduced in the mutants (49.2±2.8% of controls) (Fig. 7B,C). Together, these results support a model where cerebellar BG require ERBB3 for proliferation, and that the absence of ERBB3 leads to cell-autonomous impairments in proliferation that in turn result in cerebellar lamination defects.

DISCUSSION

Our study provides genetic evidence for a role for ERBB3 in cerebellar development. *Erbb3* mutant mice exhibited deficits in motor coordination. Cerebellar lamination was aberrant in *GFAP::Cre;Erbb3$^{F/F}$* mice, which lack *Erbb3* in both neurons and glia of the cerebellum. Both GNs and PNs were misplaced in the mutant mice (Figs 1-3). Moreover, GNs failed to migrate into the IGL and formed ectopic clusters in the ML. The boundary between the IGL and the ML was indiscernible. These observations demonstrate that ERBB3 is necessary for cerebellar lamination. Mechanistically, ablation of the *Erbb3* gene in GNs (by *Math1::CreER^{T2}*) had no effect on GN migration (Fig. 4). Furthermore, although Cre is not expressed in PN precursors in *GFAP::Cre* mice (Anthony and Heintz, 2008; Zhuo et al., 2001), PN soma were misaligned in mutant cerebellum. These results suggest that loss of *Erbb3* in cells other than GNs and PNs contributes to the lamination defects in *GFAP::Cre;Erbb3$^{F/F}$* mice. Moreover, the number of Ki67+ cells was reduced in the PCL of *GFAP::Cre;Erbb3$^{F/F}$* mice, suggesting that BG proliferation was reduced (Fig. 7). Finally, ERBB3 was expressed in cerebellar astroglial cells and was required for their proliferation in culture (Figs 4 and 6). These observations support a working model where cerebellar BG require ERBB3 for proliferation. Diminished BG proliferation in the absence of ERBB3 causes reduction and disorganization of BG scaffold, that is required for GN migration and cerebellar lamination.

ERBB3 is important for morphogenesis of different organs and tissues, including the heart, pancreas, adrenal gland, mammary

Development (2015) 142, 1-11 doi:10.1242/dev.115931

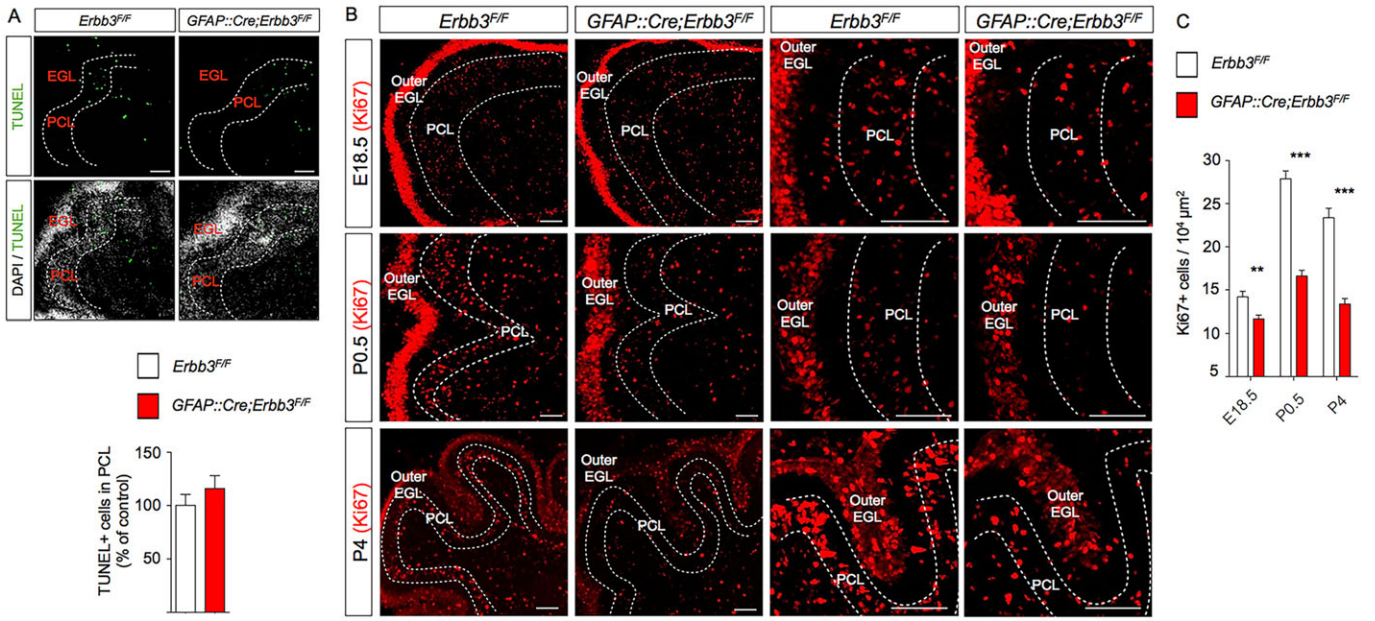

Fig. 7. The number of proliferative cells is reduced in the PCL of *Erbb3* mutant cerebella. (A) Similar TUNEL-labeled cells in the PCL. Fresh frozen cerebellar sections (E18.5) were subjected to TUNEL staining to reveal apoptotic cells. The PCL is outlined by dashed white lines. Scale bars: 100 µm. TUNEL+ cells in the PCL were quantified (n=80 folia from four controls, 56 folia from three mutants; P=0.32; t-test). (B) Decreased proliferation of BG in *Erbb3* mutant mice. Coronal cerebellar sections at E18.5, P0.5 and P4 were subjected to anti-Ki67 immunostaining to reveal proliferating cells in the PCL (outlined by dashed white lines). The right columns show images at high magnification for each genotype. Data are representative of results obtained from three mice per group. Scale bars: 100 µm. (C) Ki67+ cells in PCL in A were quantified. Data were analyzed by Student t-test (E18.5, n=30 images from three animals per genotype, $^{**}P$<0.01; P0.5, n=48 images from three controls and 50 images from three mutants, $^{***}P$<0.0001; P4, n=10 images from three controls and seven images from three mutants; $^{***}P$<0.0001). Data are mean±s.e.m.

gland and peripheral nervous system (PNS) (Erickson et al., 1997; Jackson-Fisher et al., 2008; Riethmacher et al., 1997). Most *Erbb3*-null embryos die at E13.5 due to cardiac defects and display defects in the midbrain/hindbrain region, including the cerebellum (Erickson et al., 1997). *Erbb3*-null mice that are born die soon after birth from death of sensory and motor neurons, presumably due to impaired survival or proliferation of Schwann cell precursors (SCPs) (Lyons et al., 2005; Riethmacher et al., 1997). ERBB3 has been implicated in myelination in the PNS as well as the CNS (Brinkmann et al., 2008; Makinodan et al., 2012). *Nrg1*-null embryos exhibit cardiac defects, similar to *Erbb3*-null embryos; mice lacking *Nrg1* in motor neurons display motor neuron death, and myelination defects in the PNS (Brinkmann et al., 2008; Erickson et al., 1997; Yang et al., 2001). Because of embryonic lethality of *Nrg1*-null mutation, understanding of NRG1-ERBB signaling in CNS development came mostly from *in vitro* and explant studies. In one model, NRG1 promotes radial migration of neurons in the cerebellum and cerebrum by stimulating ERBB kinases in BG and radial glial cells, respectively (Anton et al., 1997; Rio et al., 1997). However, double mutation of *Erbb2* and *Erbb4*, the two ERBBs with active kinase domains and whose kinase activity can be stimulated by NRG1 (Holmes et al., 1992; Plowman et al., 1993), by *GFAP::Cre* did not reveal morphological abnormalities in the cerebellum and cerebrum (Barros et al., 2009). These observations suggest that the NRG1 signaling pathway may not be necessary for cortical lamination. In agreement, knockout of *Nrg1* by *GFAP::Cre* had no effect on cerebellar lamination (data not shown).

In addition to NRG1, two other NRG proteins, NRG2 and NRG6, bind to ERBB3 and are expressed in the cerebellum (Aono et al., 2000; Busfield et al., 1997; Carraway et al., 1997; Juttner et al., 2005; Kinugasa et al., 2004). Moreover, recent data suggest that ERBB3 possesses some intrinsic kinase activity for auto-phosphorylation, albeit 1000-fold less active than EGFR (Shi et al., 2010). It is unknown whether ERBB3 is regulated by a NRG ligand. *Nrg2*- and *Nrg6*-null mice are viable without apparent deficits in cerebellar lamination (Britto et al., 2004; Juttner et al., 2005), probably due to functional redundancy of NRGs. The existence of multiple NRG ligands for ERBB3 suggests functional redundancy, which adds a layer of complexity in delineating the role of each NRG in neural development. Adding to the complexity is the fact that ERBB3 may dimerize with ERBB2 and ERBB4 (Berger et al., 2004). However, previous studies have shown that ERBB2 and ERBB4 are dispensable for cerebellar lamination (Barros et al., 2009; Gajendran et al., 2009). Therefore, ERBB3 regulation of cerebellar lamination may be independent of other ERBBs. Double or triple mutation of different NRGs may be necessary to unravel the role of NRGs in cerebellar development.

PI3K activation has been implicated in ERBB3-dependent proliferation and survival of various cancer cells (Cook et al., 2011; Smirnova et al., 2012; Young et al., 2013). ERBB3 contains seven binding motifs for PI3K, in contrast to one in ERBB4 and none in EGFR and ERBB2 (Schulze et al., 2005; Soltoff et al., 1994). Deletion of *Pten*, a negative regulator of PI3K-AKT signaling, results in cerebellar lamination deficits (Marino et al., 2002; Yue et al., 2005), suggesting that normal levels of PI3K-AKT activity are important for cerebellar lamination. GRB2, an adaptor protein, can bind to two phosphorylated tyrosine residues in the ICD of ERBB3 and activate the MAPK signaling cascade, which has been implicated in proliferation of glial cells (Fischer et al., 2009; Schulze et al., 2005; Zhang and Liu, 2002). Moreover, the adaptor CRK has high affinity for pY1276 in the ICD of ERBB3. Loss of CRK and/or reduced phosphorylation of CRK leads to abnormal lamination of the cerebellar cortex (Park and Curran, 2008; Jones et al., 2006;

Development (2015) 142, 1-11 doi:10.1242/dev.115931

Qiu et al., 2010). Intriguingly, levels of pAKT, pERK and pCRK in cerebellar lysates were similar between control and *Erbb3* mutant pups (supplementary material Fig. S6), suggesting that these signaling pathways may be dispensable for ERBB3-mediated BG proliferation.

Previous studies suggest that proliferation and survival of astrocytes and neural precursors requires FGF (fibroblast growth factor) signaling (Kang and Song, 2010; Morrison and de Vellis, 1981). Interestingly, ERBB3 is required for FGFR2-dependent proliferation of cancer cells (Kunii et al., 2008). ERBB3 may act together with FGF signaling to regulate cerebellar lamination. In support of this notion are observations that conditional knockout of *Fgf9* or double knockout of two FGF receptors (FGFR1 and FGFR2) causes cerebellar deficits similar to those observed in *Erbb3* mutants (Lin et al., 2009).

In conclusion, our study establishes an essential role for ERBB3 in cerebellar lamination, identifying a novel function of *Erbb3* in BG proliferation, an important step during cerebellar development. Our study demonstrates that cerebellar astroglia, including BG, require ERBB3 for proliferation. In the absence of ERBB3, BG fail to proliferate and thus cause insufficient scaffolding for GN migration, a process that is essential for cerebellar lamination.

MATERIALS AND METHODS

Generation of mice

Erbb3$^{F/F}$ (SV129/C57BL) mice were crossed with *GFAP::Cre* (FVB/J) or *Math1::CreER*^{T2} (FVB/J) mice (Machold and Fishell, 2005; Qu et al., 2006; Zhuo et al., 2001). All mice were housed in a room at 23°C in a 12 h light/dark cycle with access to food and water *ad libitum*. *Math1::CreER*^{T2} was activated by injecting pregnant dams intraperitoneally (i.p.) once with tamoxifen at 4 mg/35 g mouse. PCR-based genotyping was performed on tail genomic DNA. The following primers were used: *GFAP::Cre* (forward, ACTCCTTCATAAAGCCCTCG; reverse, ATCACTCGTTGCATCGACCG); floxed *Erbb3* allele (forward, GGCAGGCATGTTGACTTCACTTGT; reverse, CCAACCCTTCTCCTCAGATAGG); wild-type *Erbb3* allele (forward, TGTTTGTGAAATGTGGACTTTACC; reverse, CCAACCCTTCTCCTCAGATAGG); *Math1::CreER*^{T2} allele (forward, GCGGTCTGGCAGTAAAAACTATC; reverse, GTGAAACAGCATTGCTGTCACTT). Experimental procedures were approved by the Institutional Animal Care and Use Committee of Georgia Regents University.

Western blotting

Western blotting was performed as described previously (Barik et al., 2014; Shen et al., 2013; Yin et al., 2013a). Brain tissues were homogenized in RIPA buffer containing 50 mM Tris-HCl (pH 7.4), 150 mM NaCl, 2 mM EDTA, 1% sodium deoxycholate, 1% SDS, 1 mM PMSF, 50 mM NaF, 1 mM Na_3VO_4, 1 mM DTT and protease inhibitor cocktail. Debris was cleared by centrifuging samples at 12,000 ***g*** for 20 min at 4°C. Lysates were resolved by SDS-PAGE and transferred to nitrocellulose membranes (Bio-Rad) that were blocked in Tris-buffered saline (TBS) containing 0.1% Tween and 5% skim milk for 1 h at room temperature. Blocked membranes were incubated in primary antibody overnight at 4°C and then in HRP-coupled secondary antibody for 1 h at room temperature. Immunoreactive bands were visualized by enhanced chemiluminescence. The following dilutions of primary antibodies were used: rabbit anti-ERBB3 (1:500, sc-285, Santa-Cruz), rabbit anti-ERBB3 (1:100, 12708S, Cell Signaling), mouse anti-α-tubulin (1:5000, sc-23948, Santa Cruz), mouse anti-CRK (1:1000, 610035, BD Biosciences), rabbit anti-phospho CRK (1:1000, 3491, Cell Signaling), rabbit anti-AKT (1:1000, 9272, Cell Signaling), rabbit anti-pAKT (1:1000, 9271, Cell Signaling), rabbit anti-ERK (1:1000, 9102, Cell Signaling), rabbit anti-pERK (1:1000, 4377, Cell Signaling) and mouse anti-β-actin (1:1000, A1978, Sigma).

Cell culture

Granule cells and astroglia cells were purified as previously described (Hatten, 1985). Briefly, cerebella were isolated from P0 mouse pups in ice-cold phosphate-buffered saline (PBS) (Corning). After the meninges were removed, cerebella were cut into small pieces and incubated in PBS containing 0.25% trypsin (Corning) and 0.1% deoxyribonuclease (Sigma) at 37°C for 40 min. Trypsin was inactivated by incubation with DMEM (Corning) containing 10% fetal bovine serum (FBS) (Life Technologies) and penicillin-streptomycin (PS) (Hyclone). The mixture was centrifuged at 3000 rpm (500 ***g***) for 5 min. The pellet was resuspended in PBS and used for preparation of GCPs (see below) and astroglial cells. For astroglial culture, the suspended pellet was loaded on top of a two-layer Percoll (Sigma) gradient (35% Percoll and 60% Percoll in PBS) and centrifuged at 3000 rpm (1550 ***g***) for 5 min. After centrifugation, astroglial cells were collected from the top of the gradient, and recentrifuged and resuspended in DMEM containing 10% FBS and PS. The mixture of cells was passed through a 70 µm nylon filter (Falcon) to obtain a single cell suspension and pre-plated twice on uncoated 100 mm dishes (Bio-lite) for 20 min each to remove contaminant fibroblasts. Media containing unattached cells were aspirated and plated in triplicate on 12-well plates containing coverslips coated with 75 µg/ml of poly-L-lysine (Sigma) in PBS. After 4 h, fresh DMEM containing 10% FBS and PS was added to the cells. Half the media was replaced with fresh media once every 3 days.

GNs were cultured as described previously (Lee et al., 2009). Briefly, GNs were collected from the interface between the Percoll gradients, and re-centrifuged and resuspended in DMEM containing 10% FBS and PS. The mixture of cells was passed through a 40 µm nylon filter to obtain a single cell suspension and pre-plated twice on uncoated 100 mm dishes for 20 min each to remove contaminant fibroblasts. Media containing unattached cells were aspirated and plated in triplicate on 12-well plates containing coverslips coated with 500 µg/ml of poly-L-lysine (Sigma) in PBS. After 4 h, plating medium was replaced by neurobasal medium supplemented with 200 µM L-glutamine, B27 and PS. Half of the media was replaced with fresh media once every 3 days.

To prepare GCPs for adhesion assay, the cell pellet was resuspended in serum-free DMEM containing PS and passed through a 40 µm nylon filter to obtain a single cell suspension. Cells were pre-plated twice on uncoated 100 mm dishes for 20 min each to remove contaminant fibroblasts and plated in triplicates on 12-well plates containing coverslips coated with 2 µg/ml laminin (L2020, Sigma). Cerebellar microexplants were cultured as described previously (Fischer et al., 1986), with modifications. P0 cerebella were stripped of meninges and deep cerebellar nuclei, and the remaining cortical tissue was minced and suspended in PBS. The suspension was spun at 1000 rpm (150 ***g***) and the pellet was washed twice with DMEM/F12 media containing PS and plated on coverslips coated with 100 µg/ml poly-L-lysine and 10 µg/ml laminin, and maintained in DMEM/F12 media containing 20 µg/ml insulin, 1 mg/ml bovine serum albumin (BSA), 30 mM glucose, 1.8 mM glutamine, 24 mM sodium bicarbonate and PS. Coverslips were washed twice with PBS, fixed in 4% PFA and processed for immunostaining (see below).

Immunostaining

Immunostaining was performed as described previously (Yin et al., 2013a). Anesthetized mice were perfused transcardially with 4% PFA in PBS and tissues were fixed in 4% PFA at 4°C for 12 h. Frozen brain blocks were sectioned to yield 35-40 µm thick floating coronal slices. Slices were permeabilized and blocked in PBS containing 5% BSA (Sigma) and 0.3% Triton X-100 (Sigma), and incubated with primary antibodies at 4°C overnight. Primary antibodies were prepared in PBS containing 0.3% Triton X-100 by the following dilutions: mouse anti-NeuN (1:500, MAB377, Millipore), rabbit anti-ERBB3 (1:100, 12708S, Cell Signaling), mouse anti-GFAP (1:500, MAB360, Chemicon), rabbit anti-S100β (1:500, Z031129-2, Dako), rabbit anti-BLBP (1:500, ab32423, Abcam), rabbit anti-Ki67 (1:500, RM-9106-S1, Abcam), mouse anti-Tuj1 (1:500, MMS-435P, Covance), mouse anti-nestin (1:500, 556309, BD pharmingen), mouse anti-parvalbumin (1:500, PV-25, Swant) and mouse anti-calbindin (1:500, D28k-300, Swant). Slices were washed three times in PBS and incubated with Alexa Fluor-conjugated secondary antibodies (Invitrogen) for 1 h at room temperature. Slices were washed three times in PBS and mounted with VectaShield mounting medium (H-1200, Vector laboratories). TUNEL staining of fresh frozen brain sections was performed using *In Situ* Cell

Death Detection Kit (*Fluorescein*) (11684795910, Roche), following the manufacturer's instructions. Images were captured using a confocal LSM 510 NLO system (Zeiss) and processed using FIJI software.

Elevated beam-walk assay

Beam-walk assay was performed as described previously (Carter et al., 2001; Luong et al., 2011). On days 1-4, mice (3 months old) were subjected to testing on a round beam (12 mm in diameter, 1 m in length, 50 cm from the ground) (twice on days 1-2 and once on days 3-4) and latency to cross the beam was measured. On day 5, mice were tested on a square beam (5 mm in width, 80 cm in length, 50 cm from the ground). Both latency and foot slips were measured. During the tests, mice occasionally stalled while crossing the beam. They were encouraged to cross the beam by gentle prodding. However, the stalling time was not included in the readout. If a mouse was unable to the cross the beam, 60 s was entered for a particular trial.

Quantitative RT-PCR analysis

Total RNA was isolated from mouse brains using Trizol (Invitrogen) and purified using the RNeasy Mini Kit (Qiagen). Equal amounts of total RNA (4 µg) were reverse-transcribed by random hexamer primers using SuperScript III reverse transcriptase (Invitrogen). cDNA was analyzed by quantitative real-time PCR (qPCR) in triplicate using SYBR Green/ROX (Fermentas) on a Chromo 4 (Bio-Rad). mRNA levels were normalized to *Gapdh* that was assayed simultaneously on the same reaction plate. The following primers were used: *Erbb3* forward AGTGCGATTGGGACTCTG and reverse CTCCAGGTTACCCATGACCAC; *Gapdh* forward AGGTC-GGTGTGAACGGATTTG and reverse GGGGTCGTTGATGGCAACA. Products were resolved by agarose gel electrophoresis.

Statistical analysis

Statistical analyses were performed using GraphPad prism software. Data are presented as mean±s.e.m. and analyzed using Student's *t*-test, one-way ANOVA or two-way ANOVA, as appropriate. Differences among groups were considered significant if $P<0.05$. *P*-values are denoted by asterisks: $*P<0.05$; $**P<0.01$; $***P<0.001$.

Acknowledgements

We thank the Histology Core Laboratory at Georgia Regents University for assistance in Nissl staining. We thank T. W. Lin, F. Tang, X. Sun, H. Jiao and C. Bates for discussion.

Competing interests

The authors declare no competing or financial interests.

Author contributions

A.S. and L.M. designed research and wrote the paper. A.S. and A.B. performed research. A.S., A.B., D.-M.Y., C.S., J.C.B., D.F., J.-X.S., W.-C.X. analyzed data and edited manuscript.

Funding

This work was supported in part by grants from the National Institutes of Health (NIH) (W.-C.X. and L.M.). Deposited in PMC for release after 12 months.

Supplementary material

Supplementary material available online at
http://dev.biologists.org/lookup/suppl/doi:10.1242/dev.115931/-/DC1

References

Anthony, T. E. and Heintz, N. (2008). Genetic lineage tracing defines distinct neurogenic and gliogenic stages of ventral telencephalic radial glial development. *Neural Dev.* **3**, 30.

Anton, E. S., Marchionni, M. A., Lee, K. F. and Rakic, P. (1997). Role of GGF/neuregulin signaling in interactions between migrating neurons and radial glia in the developing cerebral cortex. *Development* **124**, 3501-3510.

Aono, S., Keino, H., Ono, T., Yasuda, Y., Tokita, Y., Matsui, F., Taniguchi, M., Sonta, S.-i. and Oohira, A. (2000). Genomic organization and expression pattern of mouse neuroglycan C in the cerebellar development. *J. Biol. Chem.* **275**, 337-342.

Apps, R. and Garwicz, M. (2005). Anatomical and physiological foundations of cerebellar information processing. *Nat. Rev. Neurosci.* **6**, 297-311.

Barik, A., Lu, Y., Sathyamurthy, A., Bowman, A., Shen, C., Li, L., Xiong, W. C. and Mei, L. (2014). LRP4 is critical for neuromuscular junction maintenance. *J. Neurosci.* **34**, 13892-13905.

Barros, C. S., Calabrese, B., Chamero, P., Roberts, A. J., Korzus, E., Lloyd, K., Stowers, L., Mayford, M., Halpain, S. and Muller, U. (2009). Impaired maturation of dendritic spines without disorganization of cortical cell layers in mice lacking NRG1/ErbB signaling in the central nervous system. *Proc. Natl. Acad. Sci. USA* **106**, 4507-4512.

Bean, J. C., Lin, T. W., Sathyamurthy, A., Liu, F., Yin, D. M., Xiong, W. C. and Mei, L. (2014). Genetic labeling reveals novel cellular targets of schizophrenia susceptibility gene: distribution of GABA and non-GABA ErbB4-positive cells in adult mouse brain. *J. Neurosci.* **34**, 13549-13566.

Ben-Arie, N., Bellen, H. J., Armstrong, D. L., McCall, A. E., Gordadze, P. R., Guo, Q., Matzuk, M. M. and Zoghbi, H. Y. (1997). Math1 is essential for genesis of cerebellar granule neurons. *Nature* **390**, 169-172.

Berger, M. B., Mendrola, J. M. and Lemmon, M. A. (2004). ErbB3/HER3 does not homodimerize upon neuregulin binding at the cell surface. *FEBS Lett.* **569**, 332-336.

Bignami, A. and Dahl, D. (1973). Differentiation of astrocytes in the cerebellar cortex and the pyramidal tracts of the newborn rat. An immunofluorescence study with antibodies to a protein specific to astrocytes. *Brain Res.* **49**, 393-402.

Brinkmann, B. G., Agarwal, A., Sereda, M. W., Garratt, A. N., Müller, T., Wende, H., Stassart, R. M., Nawaz, S., Humml, C., Velanac, V. et al. (2008). Neuregulin-1/ErbB signaling serves distinct functions in myelination of the peripheral and central nervous system. *Neuron* **59**, 581-595.

Britto, J. M., Lukehurst, S., Weller, R., Fraser, C., Qiu, Y., Hertzog, P. and Busfield, S. J. (2004). Generation and characterization of neuregulin-2-deficient mice. *Mol. Cell. Biol.* **24**, 8221-8226.

Buckner, R. L. (2013). The cerebellum and cognitive function: 25 years of insight from anatomy and neuroimaging. *Neuron* **80**, 807-815.

Busfield, S. J., Michnick, D. A., Chickering, T. W., Revett, T. L., Ma, J., Woolf, E. A., Comrack, C. A., Dussault, B. J., Woolf, J., Goodearl, A. D. et al. (1997). Characterization of a neuregulin-related gene, Don-1, that is highly expressed in restricted regions of the cerebellum and hippocampus. *Mol. Cell. Biol.* **17**, 4007-4014.

Carraway, K. L., III, Weber, J. L., Unger, M. J., Ledesma, J., Yu, N., Gassmann, M. and Lai, C. (1997). Neuregulin-2, a new ligand of ErbB3/ErbB4-receptor tyrosine kinases. *Nature* **387**, 512-516.

Carter, R. J., Morton, J. and Dunnett, S. B. (2001). Motor coordination and balance in rodents. *Curr. Protoc. Neurosci.* Chapter 8, Unit 8 12.

Celio, M. R. (1990). Calbindin D-28k and parvalbumin in the rat nervous system. *Neuroscience* **35**, 375-475.

Cook, R. S., Garrett, J. T., Sanchez, V., Stanford, J. C., Young, C., Chakrabarty, A., Rinehart, C., Zhang, Y., Wu, Y., Greenberger, L. et al. (2011). ErbB3 ablation impairs PI3K/Akt-dependent mammary tumorigenesis. *Cancer Res.* **71**, 3941-3951.

Cui, W., Allen, N. D., Skynner, M., Gusterson, B. and Clark, A. J. (2001). Inducible ablation of astrocytes shows that these cells are required for neuronal survival in the adult brain. *Glia* **34**, 272-282.

Delaney, C. L., Brenner, M. and Messing, A. (1996). Conditional ablation of cerebellar astrocytes in postnatal transgenic mice. *J. Neurosci.* **16**, 6908-6918.

Engelkamp, D., Rashbass, P., Seawright, A. and van Heyningen, V. (1999). Role of Pax6 in development of the cerebellar system. *Development* **126**, 3585-3596.

Erickson, S. L., O'Shea, K. S., Ghaboosi, N., Loverro, L., Frantz, G., Bauer, M., Lu, L. H. and Moore, M. W. (1997). ErbB3 is required for normal cerebellar and cardiac development: a comparison with ErbB2-and heregulin-deficient mice. *Development* **124**, 4999-5011.

Fatemi, S. H., Aldinger, K. A., Ashwood, P., Bauman, M. L., Blaha, C. D., Blatt, G. J., Chauhan, A., Chauhan, V., Dager, S. R., Dickson, P. E. et al. (2012). Consensus paper: pathological role of the cerebellum in autism. *Cerebellum* **11**, 777-807.

Fazzari, P., Paternain, A. V., Valiente, M., Pla, R., Luján, R., Lloyd, K., Lerma, J., Marín, O. and Rico, B. (2010). Control of cortical GABA circuitry development by Nrg1 and ErbB4 signalling. *Nature* **464**, 1376-1380.

Feng, L., Hatten, M. E. and Heintz, N. (1994). Brain lipid-binding protein (BLBP): a novel signaling system in the developing mammalian CNS. *Neuron* **12**, 895-908.

Fischer, G., Kunemund, V. and Schachner, M. (1986). Neurite outgrowth patterns in cerebellar microexplant cultures are affected by antibodies to the cell surface glycoprotein L1. *J. Neurosci.* **6**, 605-612.

Fischer, A. J., Scott, M. A. and Tuten, W. (2009). Mitogen-activated protein kinase-signaling stimulates Müller glia to proliferate in acutely damaged chicken retina. *Glia* **57**, 166-181.

Gajendran, N., Kapfhammer, J. P., Lain, E., Canepari, M., Vogt, K., Wisden, W. and Brenner, H. R. (2009). Neuregulin signaling is dispensable for NMDA- and GABA(A)-receptor expression in the cerebellum in vivo. *J. Neurosci.* **29**, 2404-2413.

Goldowitz, D. and Hamre, K. (1998). The cells and molecules that make a cerebellum. *Trends Neurosci.* **21**, 375-382.

Hatten, M. E. (1985). Neuronal regulation of astroglial morphology and proliferation in vitro. *J. Cell Biol.* **100**, 384-396.

Holmes, W. E., Sliwkowski, M. X., Akita, R. W., Henzel, W. J., Lee, J., Park, J. W., Yansura, D., Abadi, N., Raab, H., Lewis, G. D. et al. (1992). Identification of heregulin, a specific activator of p185erbB2. *Science* **256**, 1205-1210.

Jackson-Fisher, A. J., Bellinger, G., Breindel, J. L., Tavassoli, F. A., Booth, C. J., Duong, J. K. and Stern, D. F. (2008). ErbB3 is required for ductal morphogenesis in the mouse mammary gland. *Breast Cancer Res.* **10**, R96.
Jones, R. B., Gordus, A., Krall, J. A., and MacBeath, G. (2006). A quantitative protein interaction network for the ErbB receptors using protein microarrays. *Nature* **439**, 168-174.
Jüttner, R., Moré, M. I., Das, D., Babich, A., Meier, J., Henning, M., Erdmann, B., Müller, E.-C., Otto, A., Grantyn, R. et al. (2005). Impaired synapse function during postnatal development in the absence of CALEB, an EGF-like protein processed by neuronal activity. *Neuron* **46**, 233-245.
Kang, K. and Song, M.-R. (2010). Diverse FGF receptor signaling controls astrocyte specification and proliferation. *Biochem. Biophys. Res. Commun.* **395**, 324-329.
Kinugasa, Y., Ishiguro, H., Tokita, Y., Oohira, A., Ohmoto, H. and Higashiyama, S. (2004). Neuroglycan C, a novel member of the neuregulin family. *Biochem. Biophys. Res. Commun.* **321**, 1045-1049.
Koirala, S., Jin, Z., Piao, X. and Corfas, G. (2009). GPR56-regulated granule cell adhesion is essential for rostral cerebellar development. *J. Neurosci.* **29**, 7439-7449.
Komuro, H. and Yacubova, E. (2003). Recent advances in cerebellar granule cell migration. *Cell. Mol. Life Sci.* **60**, 1084-1098.
Kunii, K., Davis, L., Gorenstein, J., Hatch, H., Yashiro, M., Di Bacco, A., Elbi, C. and Lutterbach, B. (2008). FGFR2-amplified gastric cancer cell lines require FGFR2 and Erbb3 signaling for growth and survival. *Cancer Res.* **68**, 2340-2348.
Laure-Kamionowska, M. and Maslinska, D. (2007). Astroglia and microglia in cerebellar neuronal migration disturbances. *Folia Neuropathol.* **45**, 205-212.
Lee, H. Y., Greene, L. A., Mason, C. A. and Manzini, M. C. (2009). Isolation and culture of post-natal mouse cerebellar granule neuron progenitor cells and neurons. *J. Vis. Exp.* **23**, 990.
Li, P., Du, F., Yuelling, L. W., Lin, T., Muradimova, R. E., Tricarico, R., Wang, J., Enikolopov, G., Bellacosa, A., Wechsler-Reya, R. J. et al. (2013). A population of Nestin-expressing progenitors in the cerebellum exhibits increased tumorigenicity. *Nat. Neurosci.* **16**, 1737-1744.
Lin, Y., Chen, L., Lin, C., Luo, Y., Tsai, R. Y. and Wang, F. (2009). Neuron-derived FGF9 is essential for scaffold formation of Bergmann radial fibers and migration of granule neurons in the cerebellum. *Dev. Biol.* **329**, 44-54.
Luong, T. N., Carlisle, H. J., Southwell, A. and Patterson, P. H. (2011). Assessment of motor balance and coordination in mice using the balance beam. *J. Vis. Exp.* **49**, 2376.
Lyons, D. A., Pogoda, H.-M., Voas, M. G., Woods, I. G., Diamond, B., Nix, R., Arana, N., Jacobs, J. and Talbot, W. S. (2005). erbb3 and erbb2 are essential for schwann cell migration and myelination in zebrafish. *Curr. Biol.* **15**, 513-524.
Machold, R. and Fishell, G. (2005). Math1 is expressed in temporally discrete pools of cerebellar rhombic-lip neural progenitors. *Neuron* **48**, 17-24.
Makinodan, M., Rosen, K. M., Ito, S. and Corfas, G. (2012). A critical period for social experience-dependent oligodendrocyte maturation and myelination. *Science* **337**, 1357-1360.
Manni, E. and Petrosini, L. (2004). A century of cerebellar somatotopy: a debated representation. *Nat. Rev. Neurosci.* **5**, 241-249.
Marino, S., Krimpenfort, P., Leung, C., van der Korput, H. A., Trapman, J., Camenisch, I., Berns, A. and Brandner, S. (2002). PTEN is essential for cell migration but not for fate determination and tumourigenesis in the cerebellum. *Development* **129**, 3513-3522.
Mei, L. and Nave, K.-A. (2014). Neuregulin-ERBB signaling in the nervous system and neuropsychiatric diseases. *Neuron* **83**, 27-49.
Mei, L. and Xiong, W. C. (2008). Neuregulin 1 in neural development, synaptic plasticity and schizophrenia. *Nat. Rev. Neurosci.* **9**, 437-452.
Morrison, R. S. and de Vellis, J. (1981). Growth of purified astrocytes in a chemically defined medium. *Proc. Natl. Acad. Sci. USA* **78**, 7205-7209.
Park, T.-J. and Curran, T. (2008). Crk and Crk-like play essential overlapping roles downstream of disabled-1 in the Reelin pathway. *J. Neurosci.* **28**, 13551-13562.
Peng, Y.-J., He, W.-Q., Tang, J., Tao, T., Chen, C., Gao, Y.-Q., Zhang, W.-C., He, X.-Y., Dai, Y.-Y., Zhu, N.-C. et al. (2010). Trio is a key guanine nucleotide exchange factor coordinating regulation of the migration and morphogenesis of granule cells in the developing cerebellum. *J. Biol. Chem.* **285**, 24834-24844.
Plowman, G. D., Green, J. M., Culouscou, J.-M., Carlton, G. W., Rothwell, V. M. and Buckley, S. (1993). Heregulin induces tyrosine phosphorylation of HER4/p180erbB4. *Nature* **366**, 473-475.
Poretti, A., Prayer, D. and Boltshauser, E. (2009). Morphological spectrum of prenatal cerebellar disruptions. *Eur. J. Paediatr. Neurol.* **13**, 397-407.
Qiu, Z., Cang, Y. and Goff, S. P. (2010). Abl family tyrosine kinases are essential for basement membrane integrity and cortical lamination in the cerebellum. *J. Neurosci.* **30**, 14430-14439.
Qu, Q. and Smith, F. I. (2005). Neuronal migration defects in cerebellum of the Largemyd mouse are associated with disruptions in Bergmann glia organization and delayed migration of granule neurons. *Cerebellum* **4**, 261-270.
Qu, S., Rinehart, C., Wu, H.-H., Wang, S. E., Carter, B., Xin, H., Kotlikoff, M. and Arteaga, C. L. (2006). Gene targeting of ErbB3 using a Cre-mediated unidirectional DNA inversion strategy. *Genesis* **44**, 477-486.
Rakic, P. (1971). Neuron-glia relationship during granule cell migration in developing cerebellar cortex. A Golgi and electronmicroscopic study in Macacus Rhesus. *J. Comp. Neurol.* **141**, 283-312.
Riethmacher, D., Sonnenberg-Riethmacher, E., Brinkmann, V., Yamaai, T., Lewin, G. R. and Birchmeier, C. (1997). Severe neuropathies in mice with targeted mutations in the ErbB3 receptor. *Nature* **389**, 725-730.
Rio, C., Rieff, H. I., Qi, P. and Corfas, G. (1997). Neuregulin and erbB receptors play a critical role in neuronal migration. *Neuron* **19**, 39-50.
Rorke, L. B., Fogelson, M. H. and Riggs, H. E. (1968). Cerebellar heterotopia in infancy. *Dev. Med. Child Neurol.* **10**, 644-650.
Schulze, W. X., Deng, L. and Mann, M. (2005). Phosphotyrosine interactome of the ErbB-receptor kinase family. *Mol. Syst. Biol.* **1**, 2005.0008.
Shen, C., Lu, Y., Zhang, B., Figueiredo, D., Bean, J., Jung, J., Wu, H., Barik, A., Yin, D.-M., Xiong, W.-C. et al. (2013). Antibodies against low-density lipoprotein receptor-related protein 4 induce myasthenia gravis. *J. Clin. Invest.* **123**, 5190-5202.
Shi, F., Telesco, S. E., Liu, Y., Radhakrishnan, R. and Lemmon, M. A. (2010). ErbB3/HER3 intracellular domain is competent to bind ATP and catalyze autophosphorylation. *Proc. Natl. Acad. Sci. USA* **107**, 7692-7697.
Smirnova, T., Zhou, Z. N., Flinn, R. J., Wyckoff, J., Boimel, P. J., Pozzuto, M., Coniglio, S. J., Backer, J. M., Bresnick, A. R., Condeelis, J. S. et al. (2012). Phosphoinositide 3-kinase signaling is critical for ErbB3-driven breast cancer cell motility and metastasis. *Oncogene* **31**, 706-715.
Soltoff, S. P., Carraway, K. L., Ill, Prigent, S. A., Gullick, W. G. and Cantley, L. C. (1994). ErbB3 is involved in activation of phosphatidylinositol 3-kinase by epidermal growth factor. *Mol. Cell. Biol.* **14**, 3550-3558.
Sotelo, C. (2004). Cellular and genetic regulation of the development of the cerebellar system. *Prog. Neurobiol.* **72**, 295-339.
Soto-Ares, G., Delmaire, C., Deries, B., Vallee, L. and Pruvo, J. P. (2000). Cerebellar cortical dysplasia: MR findings in a complex entity. *AJNR Am. J. Neuroradiol.* **21**, 1511-1519.
Spassky, N., Han, Y.-G., Aguilar, A., Strehl, L., Besse, L., Laclef, C., Ros, M. R., Garcia-Verdugo, J. M. and Alvarez-Buylla, A. (2008). Primary cilia are required for cerebellar development and Shh-dependent expansion of progenitor pool. *Dev. Biol.* **317**, 246-259.
Ting, A. K., Chen, Y., Wen, L., Yin, D.-M., Shen, C., Tao, Y., Liu, X., Xiong, W.-C. and Mei, L. (2011). Neuregulin 1 promotes excitatory synapse development and function in GABAergic interneurons. *J. Neurosci.* **31**, 15-25.
Wang, V. Y. and Zoghbi, H. Y. (2001). Genetic regulation of cerebellar development. *Nat. Rev. Neurosci.* **2**, 484-491.
Weyer, A. and Schilling, K. (2003). Developmental and cell type-specific expression of the neuronal marker NeuN in the murine cerebellum. *J. Neurosci. Res.* **73**, 400-409.
Yamada, K. and Watanabe, M. (2002). Cytodifferentiation of Bergmann glia and its relationship with Purkinje cells. *Anat. Sci. Int.* **77**, 94-108.
Yang, X., Arber, S., William, C., Li, L., Tanabe, Y., Jessell, T. M., Birchmeier, C. and Burden, S. J. (2001). Patterning of muscle acetylcholine receptor gene expression in the absence of motor innervation. *Neuron* **30**, 399-410.
Yang, J.-M., Zhang, J., Chen, X.-J., Geng, H.-Y., Ye, M., Spitzer, N. C., Luo, J.-H., Duan, S.-M. and Li, X.-M. (2013). Development of GABA circuitry of fast-spiking basket interneurons in the medial prefrontal cortex of erbb4-mutant mice. *J. Neurosci.* **33**, 19724-19733.
Yin, D.-M., Chen, Y.-J., Lu, Y.-S., Bean, J. C., Sathyamurthy, A., Shen, C., Liu, X., Lin, T. W., Smith, C. A., Xiong, W.-C. et al. (2013a). Reversal of behavioral deficits and synaptic dysfunction in mice overexpressing neuregulin 1. *Neuron* **78**, 644-657.
Yin, D.-M., Sun, X.-D., Bean, J. C., Lin, T. W., Sathyamurthy, A., Xiong, W.-C., Gao, T.-M., Chen, Y.-J. and Mei, L. (2013b). Regulation of spine formation by ErbB4 in PV-positive interneurons. *J. Neurosci.* **33**, 19295-19303.
Young, C. D., Pfefferle, A. D., Owens, P., Kuba, M. G., Rexer, B. N., Balko, J. M., Sanchez, V., Cheng, H., Perou, C. M., Zhao, J. J. et al. (2013). Conditional loss of ErbB3 delays mammary gland hyperplasia induced by mutant PIK3CA without affecting mammary tumor latency, gene expression, or signaling. *Cancer Res.* **73**, 4075-4085.
Yue, Q., Groszer, M., Gil, J. S., Berk, A. J., Messing, A., Wu, H. and Liu, X. (2005). PTEN deletion in Bergmann glia leads to premature differentiation and affects laminar organization. *Development* **132**, 3281-3291.
Zhang, W. and Liu, H. T. (2002). MAPK signal pathways in the regulation of cell proliferation in mammalian cells. *Cell Res.* **12**, 9-18.
Zhuo, L., Theis, M., Alvarez-Maya, I., Brenner, M., Willecke, K. and Messing, A. (2001). hGFAP-cre transgenic mice for manipulation of glial and neuronal function in vivo. *Genesis* **31**, 85-94.